WILEY InterScience® DISCOVER SOMETHING GREAT

Mechanical and microstructural properties of hybrid poly(ethylene glycol)–soy protein hydrogels for wound dressing applications

Rony Snyders,[1] Kirill I. Shingel,[2] Oleg Zabeida,[1] Christophe Roberge,[2] Marie-Pierre Faure,[2] Ludvik Martinu,[1] Jolanta E. Klemberg-Sapieha[1]

[1]*Department of Engineering Physics, Ecole Polytechnique, Box 6079, Station "Centre ville", Montreal, Quebec, Canada H3C 3A7*

[2]*Bioartificial Gel Technologies Inc., 400, De Maisonneuve Ouest, Suite 1156, Montreal, Quebec, Canada H3A 1L4*

Received 8 June 2006; revised 25 September 2006; accepted 4 December 2006
Published online 22 March 2007 in Wiley InterScience (www.interscience.wiley.com). DOI: 10.1002/jbm.a.31217

Abstract: Biomimetic hydrogel made of poly(ethylene glycol) and soy protein with a water content of 96% has been developed for moist wound dressing applications. In this study, such hybrid hydrogels were investigated by both tensile and unconfined compression measurements in order to understand the relationships between structural parameters of the network, its mechanical properties and protein absorption *in vitro*. Elastic moduli were found to vary from 1 to 17 kPa depending on the composition, while the Poisson's ratio ($\approx$0.18) and deformation at break ($\approx$300%) showed no dependence on this parameter. Further calculations yielded the crosslinking concentration, the average molecular weight between crosslinks (M_C) and the mesh size. The results show that reactions between PEG and protein create polymeric chains comprising molecules of PEG and protein fragments between crosslinks. M_C is three times higher than that expected for a "theoretical network." On the basis of this data, we propose a model for the 3D network of the hydrogel, which is found to be useful for understanding drug release properties and biomedical potential of the studied material. © 2007 Wiley Periodicals, Inc. J Biomed Mater Res 83A: 88–97, 2007

Key words: PEG-based hydrogels; mechanical properties; tensile stress; unconfined compression stress; hydrogel microstructure

INTRODUCTION

Strong interest in the design and development of novel biomimetic hydrogels can be attributed to the unique combination of hydrophilicity, biocompatibility, and tissue-like properties of these materials.[1–3] Hydrogels have been suggested for numerous applications, such as controlled delivery of drugs,[4] artificial articular cartilage[5] or vessels,[6] contact lenses,[7] wound dressings,[8,9] and many other devices. Suitability of a hydrogel for a particular application often depends on the structural and mechanical characteristics of the biomaterial. For example, poly(vinyl alcohol) (PVA)-based hydrogel used to replace damaged articular cartilage has compressive moduli of 1–18 MPa,[5] whereas photopolymerized poly(ethylene glycol) (PEG)-based hydrogel for vascular vessel replacement is reported to be less stiff, with tensile moduli between 20 and 230 kPa,[6] depending on the molecular weight of PEG.

Basic mechanical properties of hydrogels determined from either tensile mode[6,10–12] or unconfined compressive measurements[5,13–15] usually include the tensile or compressive modulus, the ultimate yield and the deformation at break, respectively. Less frequently the authors also present Poisson's ratio, with the exception of the reports of Takigawa et al.[16] for polyacrylamide-based hydrogel and of Urayama et al.[17] for PVA-based hydrogel. Parameters determined in mechanical tests are frequently used to relate composition with structural organization of the material.

The hydrogel studied in this work has been developed as a hybrid material made of poly(ethylene glycol) (PEG) and natural soy protein.[2] The protein component of the hydrogel contributes to the "tissue-like"

Correspondence to: J. E. Klemberg-Sapieha; e-mail: jsapieha@polymtl.ca

Contract grant sponsors: Natural Sciences and Engineering Research Council (NSERC), Canada; Bioartificial Gel Technologies Inc., Canada

© 2007 Wiley Periodicals, Inc.

properties, whereas the bioinert polymer chains of PEG are responsible for the hydrophilicity of the material. This hydrogel contains up to 96% of water[2,18,19] and is presently used as a moist wound dressing and transdermal drug delivery device. Recent studies demonstrated that the PEG-protein hydrogel is inflammatory inert and accelerates wound closure *in vivo*.[20] Improved wound healing response is attributed to the moist environment provided by the hydrogel in the wounds and the ability of the material to interact predominantly with low-molecular weight proteins at the site of injury.[20]

Selectivity of the protein absorption *in vivo* was assumed to be governed by the pore size of the hydrogel network, but quantitative characteristics were unknown. Also, an influence of the individual components of this hybrid system on the permeability, water content, and elasticity of the biomaterial remained obscure. Therefore, in this study, we synthesized a series of hydrogels with different concentrations of soy protein and conducted a detailed characterization of their mechanical properties. Since the hydrogel reticulation appears due to formation of covalent bonds between carbonate moieties of PEG and amino groups of protein, it was expected that the variation in the concentration of protein would lead to the modification of the mechanical properties of the PEG-protein network. Special attention was devoted to the development of the hydrogel composition that would combine high water content with satisfactory mechanical performance to fulfill the requirements of stress resistance, durability, pliability, and bioactivity of the wound dressing device.

The results of the mechanical tests are interpreted in terms of crosslinking density (ν_e), mesh size (ξ), and average molecular weight between crosslinks (M_C). These structural parameters are related to the component composition of the hydrogels, which allowed us to propose a model of the structural organization of the hybrid PEG-protein material and explain its behavior in topical *in vivo* application.

EXPERIMENTAL SETUP

Synthesis of hydrogels

The hydrogels for this study were synthesized by Bioartificial Gel Technologies, Montreal, Canada. To obtain hydrogels with different compositions, protein solutions with mass concentrations (C_{Prot}) that varied from 8 to 14% were mixed with a 22% solution of PEG. The details of the hydrogel synthesis have been published elsewhere.[2,18–21] In brief, hydrogel formation is achieved via a condensation reaction between the amino groups of protein and carbonate-activated PEG with subsequent release of *p*-nitrophenol molecules. As a result of this reaction, stable urethane linkages between a biopolymer and PEG are formed. Hydrogels are then washed in a phosphate buffer solution (PBS) at pH of 7.2–7.4 to remove unreacted components. During purification, an equilibrium swelling of the hydrogel was attained. PEG used for the synthesis has a molecular weight of 8 kDa, as confirmed by ^{1}H nuclear magnetic resonance analysis (data not shown). Hydrolyzed soy protein has a relatively high polydispersity with one major component possessing a molecular weight of 45 kDa, as characterized by size-exclusion chromatography.[21]

Determination of the hydrogel composition

The determination of the protein concentration in the hydrogels after synthesis and purification ($C_{Prot/HG}$) was performed according to the following procedure. Samples of hydrogel (approximately 500 mg) were hydrolyzed in 3 mL of 1.0*M* NaOH at 60°C. After neutralization with concentrated H_3PO_4, protein-containing solutions were weighed and subjected to the bicinchoninic acid assay for protein quantification. The latter relies on the formation of Cu^{2+}-protein complex under alkaline conditions followed by reduction of Cu^{2+} to Cu^{+}. A calibration curve for protein quantification was established using standard solutions with a known concentration of hydrolyzed soy protein. The measurements were repeated in triplicate for each hydrogel composition.

After weighing swollen samples (m_s), the hydrogels were dried at 50°C for ~24 h until a constant weight (m_d) was reached. The volume fraction of polymer (crosslinked network of PEG and soy protein) in the swollen hydrogel (Φ_2) and the water content (W_c) were determined from Eqs. (1) and (2), respectively:

$$\Phi_2 = \frac{\dfrac{m_d}{\rho_d}}{\dfrac{m_d}{\rho_d} + \dfrac{(m_s - m_d)}{\rho_{Water}}} \quad (1)$$

$$W_c(\%) = 100\frac{(m_s - m_d)}{m_s}, \quad (2)$$

where ρ_d and ρ_{Water} represent the densities of dried hydrogel and water, respectively. To calculate ρ_d, we measured the thickness and the area of hydrogel samples using a micrometer, and we used the values of m_d.

Knowing $C_{Prot/HG}$ and W_C, we calculated the concentration of PEG in the hydrogel ($C_{PEG/HG}$) using the following equation:

$$C_{PEG/HG} + C_{Prot/HG} + W_c = 100\% \quad (3)$$

Evaluation of the mechanical properties

Unconfined compression mode

Mechanical properties of the hydrogels in the compression mode were measured using the Mach-1^{TM} mechanical testing system from Biosyntech, Montreal, Canada. The testing chamber was designed for uniaxial unconfined

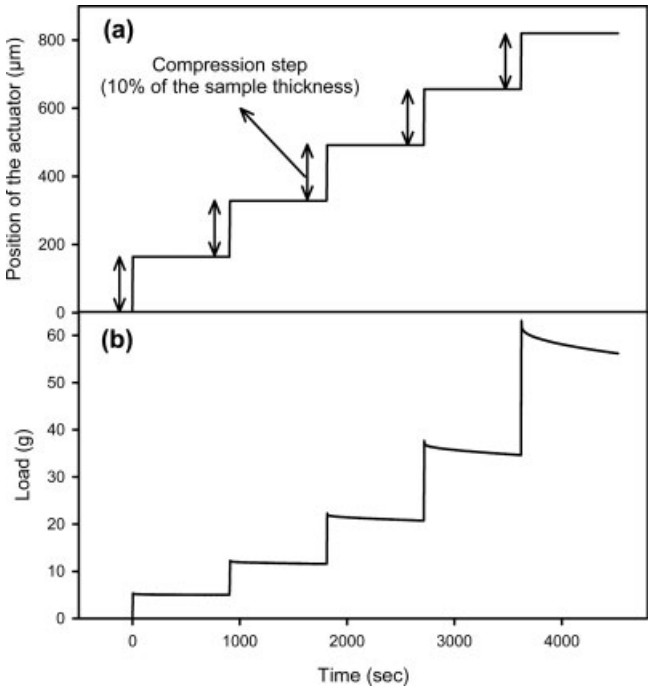

Figure 1. Typical load sequence used during the unconfined compressive measurements (a) and resulting stress–relaxation curves (b).

compression, which allows for the expansion of the swollen tablet in the radial direction and expulsion or adsorption of PBS during compression. The system consists of an actuator to precisely control the displacement with a 25 nm resolution and a load cell with a 10 mg resolution.

The samples were cut from hydrogel sheets using a 6-mm diameter punch. The diameter and the thickness of the samples were then measured using a micrometer. The relative standard deviation in these measurements was about 3%. Swollen hydrogel samples were placed on the base of the testing chamber mounted on the actuator platform. The contact between the sample and the compression post fixed to the load was precisely controlled by the displacement of the actuator until a load of 0.2 g was reached. The testing chamber was then filled with PBS solution at pH = 7.5.

For all of the measurements, the same load program has been used: the hydrogel was equilibrated for 1 h in PBS, followed by five compression steps of 10% of the sample thickness with a relaxation period of 15 min between the consecutive steps [Fig. 1(a)]. The compression rate was fixed at 35 μm/s. Assuming an elastic behavior of hydrogel and uniform strain, the compressive stress (P_C) and the strain along the thickness (ε_Z) are expressed as:

$$P_C = \frac{F}{A} \tag{4}$$

$$\varepsilon_Z = \frac{\Delta L_z}{L_z}, \tag{5}$$

where F is the force measured by the load cell, A is the area of uncompressed hydrogel sample, L_z is the initial thickness of the hydrogel sample, and ΔL_z is the deformation along the thickness. The compressive modulus after the relaxation period (E_C) is defined as the ratio of the stabilized stress over the strain:

$$E_C = \frac{P_C}{\varepsilon_Z} \tag{6}$$

At least three measurements were performed for each hydrogel composition using three separate samples.

Tensile mode

The tensile mode measurements were performed under ambient conditions using a slip-peel test instrument (Peel Tester Instrumentors SP-103B-3M45) using a load cell of 0–19 g and a displacement rate of 2.2 cm/min [Fig. 2(a)]. The hydrogel samples were cut with a punch to ensure a reproducible shape[20] in the dumbbell geometry, according to the D638-03 ASTM standard for the measurement of tensile properties of plastics. The narrow central parts of the samples were 4-cm long and 6-mm wide. The sample thickness was measured using a micrometer.

Prior to measurements, markers were drawn on the sample surface both in parallel and perpendicular to the direction of stretching (X- and Y-axis), which allowed one to measure dimension changes in both directions (Fig. 2). During the test, the tensile force was recorded by the load cell as a function of time. In addition, photographs were taken with a digital camera in 30-s intervals. The images were treated using the UTHSCSA Image Tool software, resulting in the intensity profiles along and across each sample. The markers were easily discernable as low-intensity zones. Stretching was performed until a rupture occurred, yielding the values of deformation at break (ε_u) and ultimate yield (σ_u).

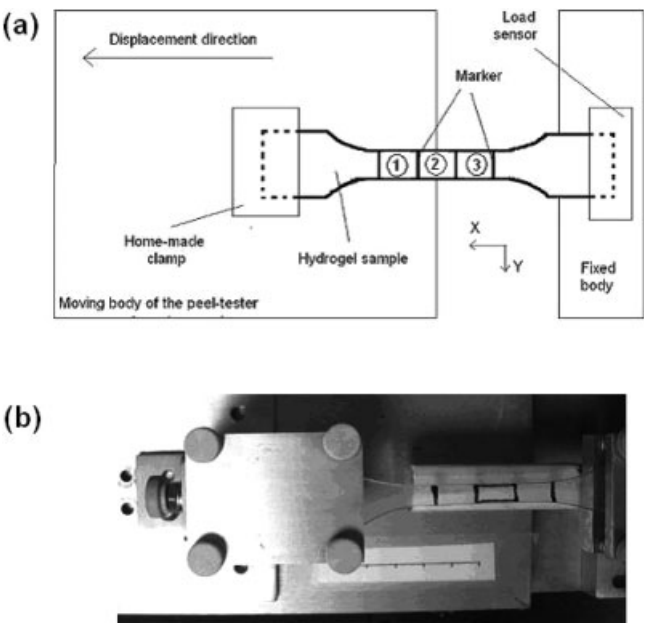

Figure 2. Experimental set-up for the tensile mode measurements.

Sample deformation (elongation along the *X*-axis and shrinking along the *Y*-axis) was calculated as a ratio of the measured and the initial distances between two markers. Elongations of segments 1–3 [Fig. 2(b)], as well as the changes in the whole central part, were evaluated for method validation purposes.

The tensile elastic modulus (E_T) and Poisson's ratio (ν) were obtained from the following relations[22]:

$$E_T = \frac{P_T}{\varepsilon_X} \tag{7}$$

$$\nu = \frac{\frac{-\varepsilon_X}{P_T}}{\frac{\varepsilon_Y}{P_T}} \tag{8}$$

where ε_X and ε_Y represent the strains in the *X*- and *Y*-directions, respectively, and P_T is the tensile stress that is calculated by dividing the tensile force by the section area of the thinner part of the dumb-bell shape sample before any deformation, as recommended by the ASTM standard.[20] Four specimens were evaluated for each hydrogel composition.

Structural properties of hydrogels

The theory of Flory for rubber elasticity allows one to quantitatively determine the characteristics of the network structure of the hydrogel. Each pair of units participating in the formation of a crosslink is selected randomly, but it requires the partners to be in suitable proximity at the moment of linkage formation.[23] Using this theory and assuming a Gaussian distribution of the chain lengths, we calculated ν_e (mol/m^3) and the average molecular weight between crosslinks, M_C, from the following equations[10,23–25]:

$$E = 3\,\nu_e \Phi_2^{1/3} RT \tag{9}$$

$$\frac{\rho_d}{M_C}\left(1 - \frac{2M_C}{M_n}\right) = \nu_e \Phi_2^{1/3}, \tag{10}$$

where E is the elastic modulus, R is the ideal gas constant (8.314 J K^{-1} mol^{-1}), M_n is the number average molecular weight of the linear polymer chain before crosslinking, and T is the temperature in Kelvin.

The microstructural characteristics of hydrogels, such as the mesh size (ξ), have been calculated, according to Temenoff et al.[26]:

$$\xi = \Phi_2^{-1/3}\left(\bar{r}_0^2\right)^{1/2} \tag{11}$$

where $\bar{r}_0^2$ is the end-to-end distance of the polymer chains. Here, the $\bar{r}_0^2$ parameter can be determined by considering the characteristic ratio of the polymer (C_n):

$$C_n = \frac{\bar{r}_0^2}{Nl^2}, \tag{12}$$

where $l = 1.47$ Å is the weighed average bond length of C—C and C—O bonds. We used $C_n = 4$ for PEG, according to Billmeyer.[27] N is the number of bonds between two crosslinks, which can be calculated from M_C for PEG:

$$N = \frac{3M_C}{M_R} \tag{13}$$

where M_R is the molecular weight of the repeating units of the chain between two crosslinks.

Protein absorption *in vitro*

This experiment was conducted to demonstrate the molecular-weight dependent mechanism of the wound proteins absorption by the PEG-protein hydrogel dressing. Small round pieces of the cotton pad were moistened with 200 μL of the PBS solution. The pads were incubated in the protein solution containing a mixture of fibrinogen (molecular weight, MW = 340 kDa), bovine serum albumin (MW = 66 kDa), soybean trypsin inhibitor (MW = 20 kDa), and aprotinin (MW = 6.5 kDa). The pads were air-dried overnight. Afterwards, the pads were covered with round pieces of hydrogels preliminarily equilibrated in the PBS overnight. Absorption of the protein from the pads proceeded for 48 h at 32°C. The samples of the hydrogel were taken after 3, 7, 24, and 48 h of incubation for protein extraction and analysis. The contact surfaces of the hydrogels were washed with PBS to remove surface-bound proteins. Analysis of the absorbed proteins was done by means of SDS electrophoresis (SDS-PAGE) of the extracts of the hydrogels in PBS.

SDS-PAGE electrophoresis under denatured conditions was done in Tris-HCl/SDS buffer on the 12% precast gels from BioRad using a constant current of 25 mA. The gels after electrophoresis were stained with Coomassie Brilliant staining solution for 2 h and then destained until a necessary degree of discoloration was obtained. Electrophoregrams were converted into numeric form using the SigmaScan software (SPSS, Chicago, IL).

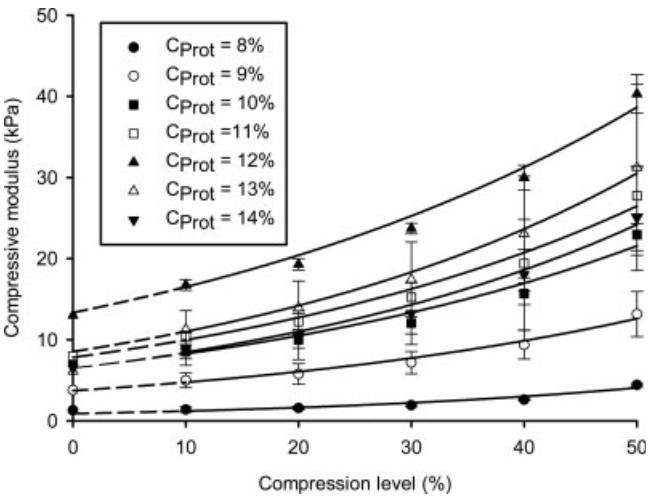

Figure 3. Compressive modulus (E_C) as a function of the level of compression for different C_{Prot}.

TABLE I
Protein ($C_{Prot/HG}$) and PEG ($C_{PEG/HG}$) Concentrations in the Hydrogel, Their Molar Content (n_{Prot}, n_{PEG}),Young's Modulus in Compression $E_{C,0}$, and Restructuring Parameter b for Hydrogels With Different Composition (C_{Prot})

C_{Prot} (%)	$C_{Prot/HG}$ (mg/g)	$C_{PEG/HG}$ (mg/g)	n_{Prot} (10^{-6} mol/cm^3)	n_{PEG} (10^{-6} mol/cm^3)	$E_{C,0}$ (kPa)	b
8	8.07 ± 2.13	32.17	0.17	4.0	0.9	0.18
9	13.37 ± 1.62	33.39	0.3	4.2	3.5	0.25
10	9.84 ± 1.45	50.99	0.22	6.3	6.1	0.63
11	12.05 ± 1.57	49.83	0.27	6.1	7.4	0.54
12	10.20 ± 0.66	55.19	0.23	7.0	12.4	0.64
13	–	–	–	–	7.6	0.51
14	8.60 ± 0.66	52.67	0.18	6.6	6.1	0.37

RESULTS

Mechanical properties of the hydrogels

Typical stress–relaxation curves obtained in the unconfined mode measurements are shown in Figure 1(b). Initially, the load increases rapidly to its maximum value corresponding to the maximum of deformation, followed by relaxation. The relaxation time increases with the level of compression. For example, for the first step, relaxation takes less than 200 s, while for the last step (50% of compression), 900 s are necessary for stabilization. Compressive modulus E_C was determined from Eq. (6) for each compression step after a relaxation time of 900 s, assuming that after this time the relaxation process was complete.

Evolution of the compressive modulus E_C as a function of the compression level is shown in Figure 3 for the hydrogels synthesized with different C_{Prot}. For all studied materials, E_C increases exponentially with stress:

$$E_C = E_{C,0} \exp(bx) \tag{14}$$

where x is the compression level. The compressive modulus at zero stress, $E_{C,0}$, and the restructuring parameter b related to the modifications of the network density due to compression[21] are determined by fitting the experimental data. The results of the analysis of the curves in Figure 3 are summarized in Table I along with the component composition of the studied materials.

Contrary to the compression tests, stress linearly increases with strain in tensile tests allowing one to determine tensile elastic modulus E_T. The method showed good reproducibility with a standard deviation below 10% for the E_T, σ_u, and ε_u values. For the Poisson ratio ν, the standard deviation can reach 25% since the measurement along both X and Y axes inevitably increases experimental errors. In every case, the hydrogel sample broke within the narrow part of the dumbbell shape, which is a necessary condition to validate the measurements. We note that the hydrogel prepared from protein solutions with a C_{Prot} lower than 9% were not sufficiently rigid to maintain the dumbbell shape.

Variation of E_T, $E_{C,0}$, and ν as a function of the protein concentration C_{Prot} in the polymerized solutions are presented in Figure 4(a,b). As can be seen, two independent techniques provided comparable values of elasticity modulus for all studied samples. Both E_T and $E_{C,0}$ were found to vary between 1 and 17 kPa, showing

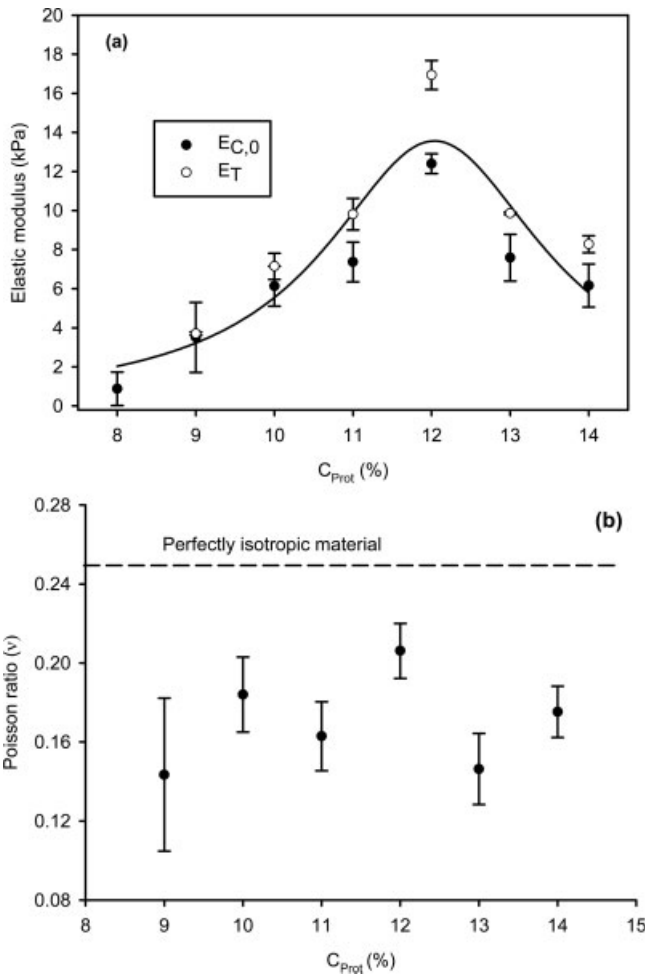

Figure 4. Evolution of the tensile (E_T) and compressive ($E_{C,0}$) elastic moduli (a) and the Poisson's ratio, ν (b) at different C_{Prot}.

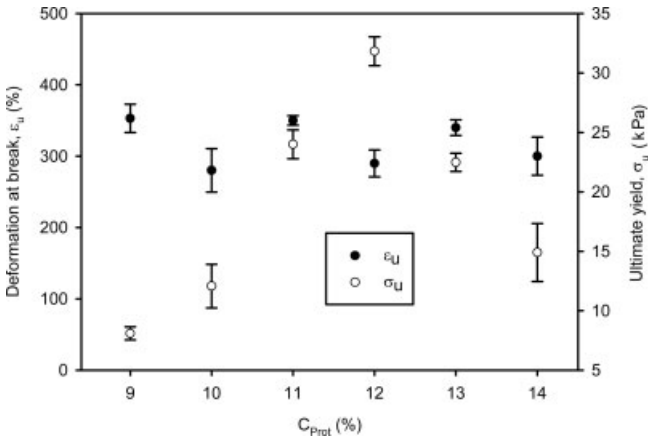

Figure 5. Evolution of the ultimate yield (σ_u) and the maximum deformation (ε_u) as a function of C_{Prot}.

maximal values of $E_T = 17$ kPa and $E_{C,0} = 12.6$ kPa for a hydrogel prepared with the $C_{Prot} = 12\%$ [Fig. 4(a)]. An increase of the C_{Prot} up to 14% does not improve the mechanical properties of the material. It was found that a solid hydrogel material could not be obtained when the concentration of soy protein exceeds 14%. Any attempts to polymerize more concentrated protein solutions failed because of poor miscibility of highly viscous solutions of both polymers.

The results of the content of the protein in the purified and completely swollen hydrogels $C_{Prot/HG}$ are reported in Table I. It is interesting to note that the values appeared to be independent of the initial concentration C_{Prot} in the polymerization solution. In contrast, the content of PEG $C_{PEG/HG}$ increases with increasing C_{Prot} and reaches maximal value at $C_{Prot} =$ 12%, similar to E_T and $E_{C,0}$.

The values of ν vary between 0.15 and 0.20 and do not show a clear dependence on C_{Prot} [Fig. 5(b)]. This observation agrees with previous publications showing that the polymer content of the networks has little effect on ν.[17] The values of ν are lower than those expected for an incompressible rubber-like material ($\nu_r = 0.5$). It is interesting to mention that close values of ν (0.15–0.35) were reported for biological tissues such as articular cartilage.[28,29]

Analysis of the ultimate deformation (Fig. 5) reveals that the deformation at break, ε_u, has the same value of about 300% for all tested samples. As a consequence, the evolution of the ultimate yield, σ_u, follows the trend observed previously for E_T and $E_{C,0}$ with the maximum value of 32 kPa at $C_{Prot} = 12\%$ (Fig. 5).

Relation between the mechanical properties and the microstructure of the hydrogel

The structural parameters of the PEG-protein hydrogels, including dried hydrogel density, ρ_d, polymer volume fraction, Φ_2, crosslinking density, ν_e, etc. are reported in Table II. In view of the fact that the elasticity moduli of the hydrogels are found to be very close in both tension and compression [Fig. 4(a)], average values between $E_{C,0}$ and E_T, denoted as E, were used for the calculations (Table II). The crosslinking density ν_e varies as a function of the C_{Prot} and has a maximal value at $C_{Prot} = 12\%$, similar to $E_{C,0}$ and E_T. Using the values of structural parameters ν_e, ρ_d, and Φ_2, we calculated molecular weight between crosslinks M_C and the mesh size of the network (ξ). The results are reported in Table III and Figure 6, which compare evolutions of ξ and the water content W_C in the hydrogels prepared with different C_{Prot}.

The calculated ν_e values are lower than those reported in other studies. For example, Lou and Van Coppenhagen[30] obtained ν_e between 4×10^{-5} and 5.16×10^{-4} mol/cm^3 for different 2-hydroxylethyl methacrylate (HEMA) gels, while Wang and Wu reported values from 10^{-4} to 1.4×10^{-3} mol/cm^3 for different copolymeric gels based on HEMA and epoxy methacrylate (EMA).[25] Comparison of the data published for different hydrogels with the parameters E and Φ_2 determined in the present work is given in Table III.

When comparing the calculated ν_e values with the molar content of PEG, it appeared that the density of effective crosslinks is lower than expected by considering the amount of the crosslinking agent (in our case, PEG) present in the hydrogel. For the hydrogel synthesized using the 12% protein solution, for exam-

TABLE II
Values of Average Elastic Modulus (E), Dried Hydrogel Density (ρ_d), Volume Fraction of the Polymer in the Swollen Hydrogels (Φ_2), Crosslinking Density (ν_e), Average Molecular Weight Between Two Crosslinks (M_C), and Mesh Size (ξ) for the Studied Hydrogel

C_{Prot} (%)	E (kPa)	ρ_d (g/cm^3)	Φ_2	ν_e (10^{-6} mol/cm^3)	M_C (kDa)	ξ (nm)
8	1.00 ± 0.16	1.42 ± 0.16	0.03	0.39	22.5	37.6
9	3.60 ± 0.09	1.35 ± 0.11	0.04	1.4	22.3	32.4
10	6.70 ± 0.57	1.64 ± 0.22	0.04	2.6	22.2	33.5
11	8.60 ± 0.65	1.21 ± 0.09	0.07	2.8	22.0	28.0
12	15.70 ± 0.46	1.42 ± 0.12	0.05	5.4	21.8	30.9
13	8.70 ± 0.08	1.17 ± 0.09	0.04	3.3	22.0	32.1
14	7.20 ± 0.36	1.61 ± 0.26	0.04	2.8	22.2	32.8

TABLE III
Comparison of Data Illustrating the Influence of Both the Elastic Modulus (*E*) and the Volume Fraction of Polymer in the Swollen Hydrogel (Φ_2) on the Crosslinking Density (ν_e)

Hydrogels	*E* (kPa)	Φ_2	ν_e (10^{-6} mol/cm^3)	Reference
HEMA/EMA copolymer	290–1097	0.52–0.80	600–16	25
Oligo(poly(ethylene glycol)fumarate)	20–100	0.30–0.35	10	26
Polyacrilamide	80	–	1400–1700	17
Poly[(acry acid)-*co*-(itaconic acid)]	8–20	0.04–0.09	3–6	16
Poly(2-hydroxyethyl methacrylate)	80–1110	0.55–0.68	40–5000	28
PEG/soy protein	1–16	0.03–0.07	0.4–6	This work

ple, 1.4×10^{17} protein molecules per cm^3 are found to be bound to 4.2×10^{18} PEG molecules (Table I), whereas the density of the crosslinks yields only 3.2×10^{18} crosslinks/cm^3. Further calculations reveal that for a total of 31 PEG molecules bound to the protein, 12 molecules are involved in the 3D elastic network, whereas 19 remaining molecules of PEG act as dangling ends and do not contribute to the elasticity of the material (Table IV). Analysis of the data presented earlier allows us to develop a microstructural model for the PEG-protein network, as schematically shown in Figure 7.

Interactions with protein *in vitro*

Previous *in vivo* studies have demonstrated that the PEG-protein wound dressing selectively absorbs small proteins from the wound bed.[20] In this work, *in vitro* protein absorption experiments were performed using fibrinogen (MW = 340 kDa), soybean trypsin inhibitor (MW = 20 kDa), bovine serum albumin (MW = 66 kDa), and aprotinin (MW = 6.5 kDa) as model compounds with known hydrodynamic dimensions. The results of this test are presented in Figure 8. After 3 h of incubation [Fig. 8(a)], serum albumin, trypsin inhibitor, and aprotinin were detected in the hydrogel. The concentration of the proteins extracted by the biomaterial increases with time [Fig. 8(b–d)]. Under denatured conditions of SDS-PAGE used here, subunits of fibrinogen should migrate with apparent molecular weights of 63.5, 56, and 47 kDa.[31] However, no bands were detected between 66 and 20 kDa, indicating that native fibrinogen used in the diffusion experiment could not penetrate into the PEG-protein matrix.

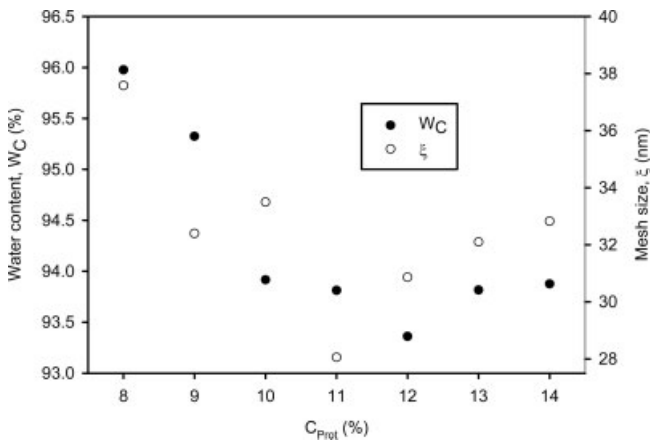

Figure 6. Effect of C_{Prot} on the mesh size (ξ) and the water content (W_C) in the hydrogels.

DISCUSSION AND CONCLUSION

In the present study, we compared the mechanical properties (elasticity moduli, Poisson's ratio, ultimate tensile yield, and deformation at break) of the PEG-protein hydrogels prepared from the solutions containing different concentrations of soy protein (C_{Prot}). It was found that the evolution of the elastic modulus and the ultimate tensile yield depends on the concentration of soy protein in the polymerized solution, though the protein content of the swollen hydrogels was rather unaffected by C_{Prot} (Table I). Elasticity of the material increases with increasing C_{Prot} from 8% to 12%. The data show that the polymerization of the 12% soy protein solution produces the strongest hydrogel (Table I). The elastic modulus and the ultimate tensile yield of this composition were found to be 15.7 and 32 kPa, respectively, at a deformation of 300%. For the hydrogels synthesized with $C_{Prot} >$ 12%, E_T and $E_{C,0}$ decrease due to low efficiency of the polymerization reaction. This interpretation is supported by the finding that the number of PEG molecules involved in the elastic network with the $C_{Prot} =$ 14% is significantly smaller than that calculated for the $C_{Prot} =$ 12% (Table IV). Indeed, when the C_{Prot} becomes high, the solution of soy protein exhibits a high viscosity, which limits its miscibility with the PEG solution and favors formation of protein aggregates. In this situation, accessibility of the individual protein molecules for crosslinking with PEG is limited, leading to a lower efficiency of network formation, and consequently, to poorer mechanical properties [Fig. 4(a)]. One may observe that both the mechanical properties and the composition of the

TABLE IV
Network Characteristics of the Hydrogel With Different C_{Prot} Expressed as the Number of PEG Molecules Bound to a Molecule of Soy Protein

C_{Prot} (%)	Number of PEG Molecules	Number of PEG Molecules Present in the Elastic Network	Number of PEG Molecules Present as Dangling Ends	Percentage of PEG Molecules Present in the Elastic Network (%)
8	22	1	21	4.8
9	14	2	12	16.4
10	29	6	23	20.5
11	23	5	18	22.8
12	31	12	19	38.3
14	35	7	27	21.2

hydrogel prepared using the 14% soy solution are comparable with those observed for the sample with $C_{Prot} = 10\%$ (Table I).

The structural properties determined from the mechanical measurements allowed us to propose a model for the hydrogel microstructure in which PEG is present in two forms: (i) PEG molecules bound to proteins by their two extremities to create a 3D elastic network, and (ii) PEG molecules bound only by one end acting as a dangling end. The proportion of dangling ends formed by PEG molecules ranges from 60 to 95%, depending on the protein concentration in the polymerized solution (Table IV). It appears from our data that the chain of molecular weight M_C (around 22 kDa) is by far larger than a molecule of PEG with a M_C of 8 kDa (Table II). This means that the chain of M_C in our hybrid hydrogel is formed by PEG molecules and fragments of the protein chain(s). In other words, a macromonomer unit of the network represents a conjugate of PEG and protein, as presented in Figure 7. As the polymerization reaction proceeds, the initially formed PEG-protein macromonomers

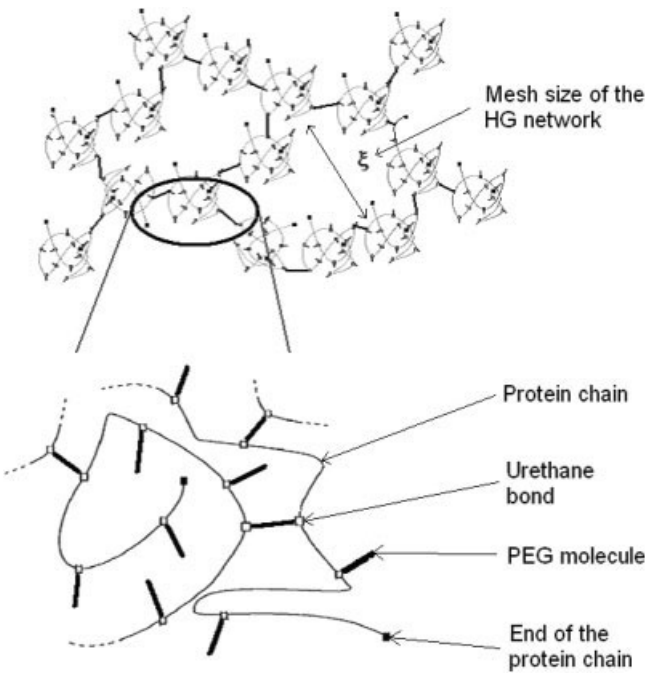

Figure 7. Microstructural model of the PEG-protein hydrogel network.

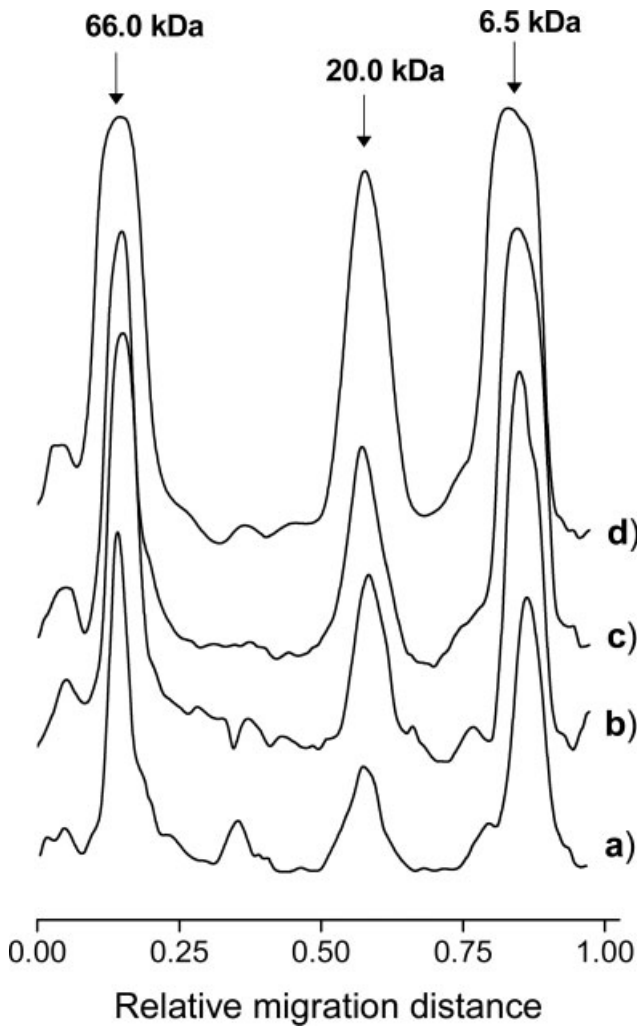

Figure 8. SDS-PAGE of the proteins (bovine serum albumin, MW = 66 kDa, soybean trypsin inhibitor, MW = 20 kDa, aprotinin, MW = 6.5 kDa) extracted from the samples of the PEG-protein hydrogel prepared with $C_{Prot} = 12\%$ after 3 h (a), 7 h (b), 24 h (c), and 48 h (d) of protein absorption *in vitro*.

further crosslink with bifunctionalized PEG, thus forming hydrogel structure with relatively large pores (Fig. 6).

Relatively low values of ν_e characterize PEG-protein hydrogel as a loosely crosslinked material, which is highly swollen in aqueous solution owing to the hydrophilic nature of both components. The values of Φ_2 (Table III) and W_C (Fig. 6) demonstrate that the studied PEG-protein hydrogel contains up to 96% of water at equilibrium. Such highly swollen structures are generally known to possess very poor mechanical resistance. In this study, however, we demonstrated that high water content could be further combined with improved mechanical properties via optimization of the polymerization reaction, as found in the hydrogel prepared with $C_{Prot} = 12\%$ (Fig. 4). A good balance between structural integrity, mechanical performance, and water content in this material predetermines its suitability for wound dressing applications.

It is known that material-tissue interactions are mediated through the so-called opsonisation mechanism comprising deposition of the protein layer on the material surface.[32] Because of the high water content, the PEG-protein hydrogel represents poor substrate for protein adsorption. In this study, we showed that a primary contact of the hydrogel with a protein-rich surface leads to *in situ* dissolution of the proteins on moist surface of the hydrogel, followed by diffusion of the small solutes in the hydrogel matrix. This observation is consistent with the previously published results showing that lightly-crosslinked PEG hydrogels hinder the absorptions of the opsonins, which render these biomaterials inflammatory inert.[33]

Comparison of the mesh size of the network with molecular dimensions of the proteins revealed that the diffusion is strictly molecular-size dependent. Serum albumin with the hydrodynamic size of 14.1 nm[34] penetrates easily 30-nm wide pores of the PEG-protein network (Table II), whereas fibrinogen (hydrodynamic size of 47 nm)[35] could not be detected in the hydrogels even after 48 h of the experiment (Fig. 8). The agreement observed between structural parameters of the network and the mechanism of the protein diffusion confirms validity of the model proposed for the microstructural organization of the hydrogel (Fig. 7). Also, these findings support the observation of the selective absorption of the relatively low molecular weight proinflammatory cytokines, i.e. IL-1b, IL-6, etc. under the conditions *in vivo*.[20]

In conclusion, the study performed on the mechanical properties of the PEG-protein hydrogel provided valuable information on the structural peculiarities and associated biological effect of this material *in vivo*. Evaluation of the influence of the PEG concentration on the structural parameters of the network can be considered as another step towards optimal design of this material for wound dressing applications.

The authors are thankful to Professor Michael Buschmann for helpful discussions and to Mr. Guillaume Plouffe for his help during the experimental work. One of us (R.S.) acknowledges the scholarship from the Belgian National Fund for Scientific Research (FNRS).

References

1. Ratner BD, Hoffman AS. Hydrogels for biomedical applications. In: Andrade JD, editor. Hydrogels for Medical and Related Applications,ACS symposium series, Vol 31. Washington, DC: American Chemical Society; 1976. p 1–36
2. Fortier G. Albumin based hydrogel. US Pat No. 5733563, 1998.
3. Giusti P, Barbani N, Lazzeri L, Lelli L. Bioartificial Polymeric Materials. J Macromol Sci Pure Appl Chem 1994; VA31 (Suppl 6/7):839–847.
4. Narayan B, Ramay HR, Gunn J, Matsen F, Zhang M. PEG-grafted chitosan as an injectable thermosensitive hydrogel for sustained protein release. J Control Release 2005;103:609–624.
5. Stammen J, Williams S, Ku DN, Guldberg RN. Mechanical properties of a novel PVA hydrogel in shear and unconfined compression. Biomaterials 2001;22:799–806.
6. Schmedlen RH, Nyugen KT, West JL. Tissue engineered vascular grafts: Elastic polyethylene glycol hydrogel scaffolds for culture under pulsatile flow conditions. Second Joint EMBS/BMES Conference, Houston, TX, USA, October 23–26, 2002. p 813–814.
7. Manetti C, Casciani L, Pescosolido N. Diffusive contribution to permeation of hydrogel contact lenses: Theoretical model and experimental evaluation by nuclear magnetic resonance techniques. Polymer 2002;43:87–92.
8. Shukla S, Bajpai AK, Kulkarni RA. Preparation, characterization, and water-sorption study of polyvinyl alcohol based hydrogels with grafted hydrophilic and hydrophobic segments. J Appl Polym Sci 2005:95:1129–1142.
9. Razzak MT, Darwis D, Zainuddin S. Irradiation of polyvinyl alcohol and polyvinyl pyrrolidone blended hydrogel for wound dressing. Radiat Phys Chem 2001;62:107–113.
10. Anseth KS, Bowman CN, Peppas LB. Mechanical properties of hydrogels and their experimental determination. Biomaterials 1996;17:1647–1657.
11. Teratsubo M, Tanaka Y, Saeki S. Measurement of stress and strain during tensile testing of gellan gum gels: Effect of deformation speed. Carbohydr Polym 2002;47:1–5.
12. Drury JL, Dennis RG, Mooney DJ. The tensile properties of alginate hydrogels. Biomaterials 2004;25:3187–3199.
13. Ravenelle F, Marchessault RH, Légaré A, Buschmann MD. Mechanical properties and structure of swollen crosslinked high amylose starch tablets. Carbohydr Polym 2002;47:259–266.
14. Rodriguez E, Katime I. Some mechanical properties of poly [(acrylic acid)-*co*-(itaconic acid)] hydrogels. Macromol Mater Eng 2003;288:607–612.
15. Muniz EC, Geuskens G. Compressive elastic modulus of polyacrylamide hydrogels and semi-IPNs with poly(*N*-isopropylacrylamide). Macromolecules 2001;34:4480–4484.
16. Takigawa T, Morino Y, Urayama K, Masuda T. Poisson's ratio of polyacrylamide (PAAm) gels. Polym Gels Networks 1996;4:1–5.
17. Urayama K, Takigawa T, Masuda T. Poisson's ratio of poly (vinyl alcohol) gels. Macromolecules 1993;26:3092–3096.
18. D'Urso EM, Fortier G. New bioartificial polymeric material: Poly(ethylene glycol) cross-linked with albumin. I. Synthesis and swelling properties. J Bio Comp Pol 1994;9:367–387.
19. Gayet JC, Fortier G. Poly(ethylene glycol) cross-linked with albumin. II. Mechanical and thermal properties. J Bio Comp Pol 1998;13:179–197.
20. Shingel KI, Di Stabille L, Marty JP, Faure MP. Inflammatory inert poly(ethylene glycol)–protein wound dressing improves

healing responses in partial- and full-thickness wounds. Int Wound J 2006;3:332–342.
21. Shingel KI, Faure MP. Structure-property relationships in poly (ethylene glycol)–protein hydrogel systems made from various proteins. Biomacromolecules 2005;6:1635–1641.
22. Standard test method for tensile properties of plastic. ASTM D638-03. West Conshohocken: ASTM. December 1, 2003.
23. Flory PJ. Principles of Polymer Chemisry. New York: Cornell University Press; 1953.
24. Peppas NA, Merrill EW. Crosslinked poly(vinyl alcohol) hydrogels as swollen elastic network. J Appl Polym Sci 1977;21:1763–1770.
25. Wang J, Wu W. Swelling behaviors, tensile properties and thermodynamic studies of water sorption of 2-hydroxyethyl methacrylate/epoxy methacrylate copolymeric hydrogels. Eur Polym J 2005;41:1143–1151.
26. Temenoff JS, Athanasiou KA, Lebaron RG, Mikos AG. Effect of poly(ethylene glycol) molecular weight on tensile and swelling properties of oligo[poly(ethylene glycol) fumarate] hydrogels for cartilage tissue engineering. J Biomed Mater Res 2002;59:429–437.
27. Billmeyer FW. Textbook of Polymer Science. New York: Wiley; 1984.
28. Roemhildt ML, Coughlin KM, Peura GD, Fleming BC, Beynnon BD. Material properties of articular cartilage in the rabbit tibial plateau. J Biomech 2006;39:2331–2337.
29. Kiviranta P, Rieppo J, Korhonen RK, Julkunen P, Töyräs J, Jurvelin JS. Collagen network primarily controls Poisson's ratio of bovine articular cartilage in compression. J Orthop Res 2006;24:690–699.
30. Lou X, Van Coppenhagen C. Mechanical characteristics of poly(2-hydroxyethyl methacrylate) hydrogels crosslinked with various difunctional compounds. Polym Int 2001;50:319–325.
31. Almany L, Seliktar D. Biosynthetic hydrogel scaffolds made from fibrinogen and polyethylene glycol for 3D cell cultures. Biomaterials 2005;26:2467–2477.
32. Tang L, Ugarova TP, Plow EF, Eaton JW. Molecular determinants of acute inflammatory responses to biomaterials. J Clin Invest 1996;97:1329–1334.
33. Krsko P, Sukhishvili S, Mansfield M, Clancy R, Libera M. Electron-beam surface patterned poly(ethylene glycol) microhydrogels. Langmuir 2003;19:5618–5625.
34. Wright KA, Thompson MB. Hydrodynamic structure of bovine serum albumin determined by transient electric birefringence. Biophys J 1975;15:137–141.
35. Serrallach EN, Hofmann VE, Zulauf M, Binkert T, Hofmann R, Kanzig W, Straub PW, Schwyzer R. Fibrinogen: Agreement of experimental and calculated hydrodynamic data with electron-microscopic models. Thromb Haemost 1979;41:648–654.